NASA
Technical
Paper
3629

October 1996

A Rolling Element Tribometer for the Study of Liquid Lubricants in Vacuum

Stephen V. Pepper, Edward Kingsbury
and Ben T. Ebihara

National Aeronautics and
Space Administration

Lewis Research Center
Cleveland, Ohio 44135

NASA Technical Paper 3629

1996

A Rolling Element Tribometer for the Study of Liquid Lubricants in Vacuum

Stephen V. Pepper
Lewis Research Center
Cleveland, Ohio

Edward Kingsbury
Interesting Rolling Contact
Walpole, Massachusetts

and

Ben T. Ebihara
Lewis Research Center
Cleveland, Ohio

National Aeronautics and Space Administration

Office of Management

Scientific and Technical Information Program

A Rolling Element Tribometer for the Study of Liquid Lubricants in Vacuum

Stephen V. Pepper
National Aeronautics and Space Administration
Lewis Research Center
Cleveland, Ohio 44135

Edward Kingsbury
Interesting Rolling Contact
Walpole, Massachusetts 02081

Ben T. Ebihara
National Aeronautics and Space Administration
Lewis Research Center
Cleveland, Ohio 44135

Summary

A tribometer for the evaluation of liquid lubricants in vacuum is described. This tribometer is essentially a thrust bearing with three balls and flat races having contact stresses and ball motions similar to those in an angular contact ball bearing operating in the boundary lubrication regime. The friction coefficient, lubrication lifetime, and species evolved from the liquid lubricant by tribodegradation can be determined. A complete analysis of the contact stresses and energy dissipation together with experimental evidence supporting the analysis are presented.

Introduction

It has long been recognized that the properties of liquids used as machinery lubricants undergo changes. Conditions such as high operating temperatures and aggressive ambient environments can lead to decomposition or can cause chemical reactions that alter the physical and chemical properties of the lubricant, possibly degrading its performance. Also, the lubricant properties can be altered simply by being subjected to tensile, compressive, and shear stresses that occur in ball bearing contacts. Liquid lubricants under such stresses and shears chemically react with the bearing surface. This tribochemical activity has been studied in the field of additive technology, which includes surface chemical reactions.

A wide range of conditions must be considered in studying liquid lubricant degradation and evolution because of the contributions of the aforementioned factors. This report describes a new instrument used to study liquid lubricant evolution and the tribological and tribochemical phenomena related to boundary lubrication in vacuum. The motivation was provided by recent experience in testing liquid-lubricated, low-speed bearings that support instruments in weather satellites. These bearings operate in the boundary lubrication regime in vacuum where darkening of the lubricant and formation of a "friction polymer" are frequently observed. The purpose of this report is to describe the instrument and the analysis of the contact conditions and to provide experimental data supporting the analysis. Subsequent reports will address the evaluation of the chemical and physical properties of specific lubricants.

The intention was to design an instrument that would exercise or stress a liquid lubricant in a manner similar to that experienced in a typical angular contact ball bearing operating in the boundary lubrication regime in vacuum. The instrument has the following characteristics:

(1) It is a rolling element tribometer operating in vacuum and at a contact stress level typically found in a preloaded angular contact ball bearing.
(2) It operates in the boundary lubrication regime.
(3) It permits a simple and rigorous analysis of the contact stresses and the energy loss to the lubricant.
(4) It enables an easy posttest examination of the tribological elements and the degraded lubricant with surface and thin-film analysis techniques.
(5) It determines the coefficient of friction.
(6) It determines the system pressure rise and allows a partial pressure analysis of the gas released by the lubricant as it degrades under tribological stress.
(7) It operates with an extremely small and finite lubricant charge to provide maximum opportunity for the lubricant molecule to be tribologically exercised and thus to undergo and exhibit tribological degradation.

The instrument provides a credible simulation of an angular contact ball bearing and serves as a screening device to aid in selecting lubricants and as a highly controlled testbed to explore issues in tribochemistry. The tribological elements of the system are shown in figure 1. Previously introduced by Kingsbury (refs. 1 and 2), the system is a retainerless steel thrust bearing with three balls placed symmetrically on flat races called plates. The top plate rotates at 4 rpm and drives the balls to roll in an almost circular orbit (approx. 21-mm or 3/16-in.

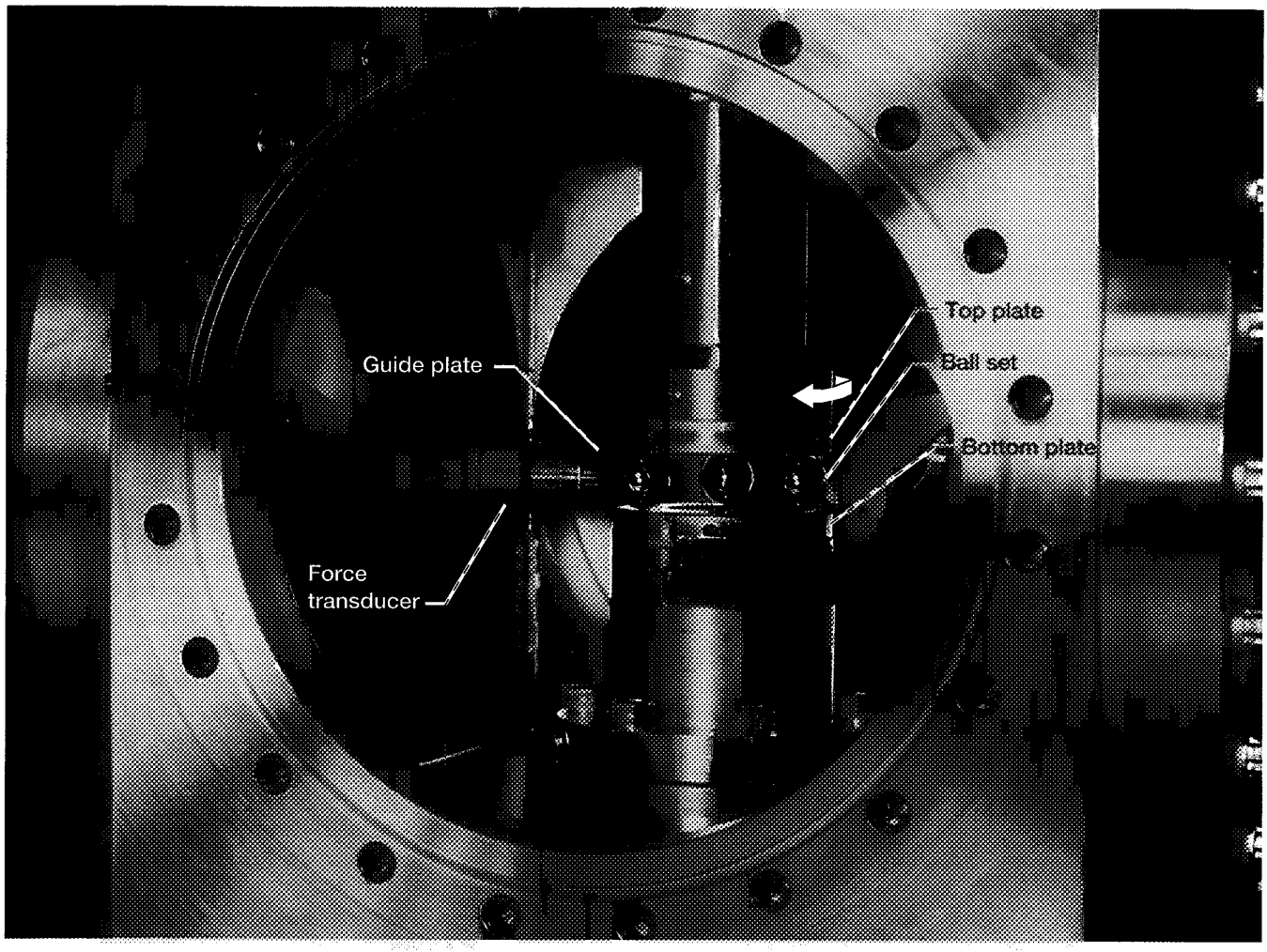

Figure 1.—Tribometer with viewport removed. Balls and plates are goldplated to facilitate recognition of triboelements.

radius) on the stationary bottom plate. The orbit is in fact a spiral—the rolling balls spiral out from their initial radii toward the edges of the plates with a pitch of approximately 0.5 mm (0.02 in.) per revolution. They would eventually fall out if allowed to continue rolling without restraint. Here, the balls contact the vertical guide plate for a short distance (approx. 5 mm or 0.2 in.) and are forced back to a smaller orbit radius. The straight-line region in which a ball contacts the guide plate is denoted herein as the scrub. This scrub proved to be beneficial in that it allowed the coefficient of friction to be measured from the force on the guide plate. After leaving the scrub, the ball's spiral orbit begins again. This final spiral orbit and the short scrub section constitute a track (fig. 2) that is stable and repeatable and is traversed thousands of times by the ball set.

A thrust bearing approach to evaluate and study lubricants was recently described by two other groups. The apparatus of C.G. Kalogeras et al. (ref. 3) uses offset grooved races operating at high speed in a vacuum with a retainer to maintain ball position. In this work, liquid lubricants have been evaluated with the emphasis on the lifetime to failure of the bearing. Lovell, Khonsari, and Marangoni (ref. 4) operated their retainerless thrust bearing with grooved races at an extremely low speed in air to explore the thin-film behavior of solid lubricants. They based an analysis of the stresses in their system on the work of Todd and Johnson (ref. 5).

An advantage of the approach described herein is that it is a more credible simulation of an angular contact instrument ball bearing operating in the boundary lubrication regime than is the usual sphere sliding on a flat in a ball-on-plate apparatus. Retainerless operation eliminates the forces associated with the ball sliding on the retainer pockets and thus allows a simple but rigorous analysis of the stress to which the lubricant is subjected. The absence of a porous retainer also eliminates the contribution it can make to enhancing the lubricant supply and to effecting chemical evolution, which have always been considered the sources of major uncertainties in understanding bearing operation. The triboelements, flat plates and commercially available balls, are not expensive and allow the instrument to be operated economically. The flat plates also make it easier to perform a surface analysis of the track after the test

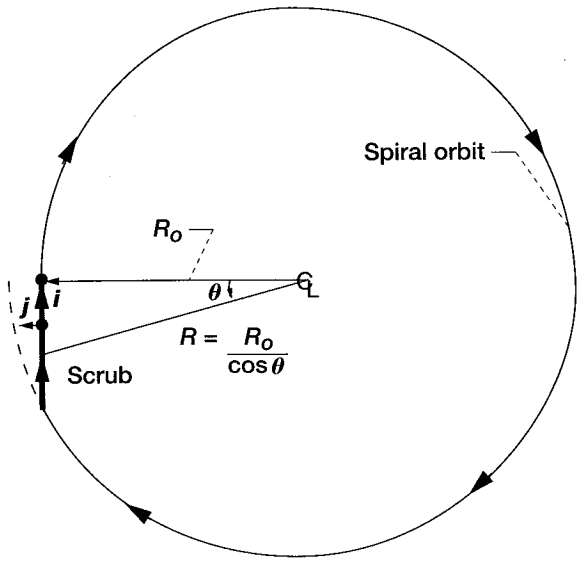

Figure 2.—Coordinate system used to analyze ball motion in scrub region. Angle included by scrub on spiral-scrub track, θ_{max} = 13.6° (determined from scrub length of 5 mm (0.2 in.) and initial orbit radius, R_o of 21 mm (13/16 in.)); radius to ball center from shaft axis, R.

than to perform one on the curved surfaces of ordinary races. Also, the instrument operating mode (low speed and cessation of motion at the first sign of increased friction) ensures against bulk temperature rise and metallic wear. Thus, material properties are always those for room-temperature conditions, and the elastic Hertz stress calculations for a sphere-on-flat geometry are always applicable. Finally, the limited amount of lubricant applied to the balls allows almost all the lubricant to be brought into the contacts thousands of times so that any tribologically induced changes can be more easily detected than when a large lubricant reservoir is available.

Experimental details of the apparatus are presented in the next section. The Analysis section contains a description of the ball motion followed by an analysis of the contact stresses and energy losses in the system. In the Results and Discussion section, the experimental results obtained with a typical liquid lubricant are shown to support the theoretical analysis and introduce some new and unexpected tribological phenomena. The report concludes with a discussion of the results and their implications for the study of liquid lubricants in rolling contacts in the boundary regime.

Symbols

A	area of contact
$\boldsymbol{F}$	friction force per unit area at a sliding contact
$\boldsymbol{i}, \boldsymbol{j}, \boldsymbol{k}$	unit vectors in an orthonormal coordinate system
m/e	mass-to-charge ratio of an ion in residual gas analyzer
n_{osc}	number of shaft revolutions in one period of a guide force oscillation
$\boldsymbol{P}$	pivot vector; the relative angular velocity of a ball and plate normal to their plane of contact
$\boldsymbol{P}_b$	pivot vector at bottom plate contact
$\boldsymbol{P}_g$	pivot vector at guide plate contact
$\boldsymbol{P}_t$	pivot vector at top plate contact
R	radius to ball center from shaft axis
R_o	radius to ball center from shaft axis for ball at scrub exit
r	radius from the center of a ball-plate contact to any point within their elastic area of contact
r_b	ball radius
r_H	radius of elastic contact area between a ball and a plate
$\boldsymbol{r}$	radius vector from ball center to any point on its surface
$\boldsymbol{r}_b$	radius vector from ball center to its top plate contact
S	severity; energy loss per unit time at a sliding contact
S_{in}	total system severity with one ball in scrub and two balls outside scrub
S_{out}	total system severity with three balls outside scrub
$\boldsymbol{V}$	linear velocity vector of top plate at ball contact
$\Delta\boldsymbol{V}$	relative linear velocity vector at contact of ball with top plate in scrub
$\boldsymbol{v}$	linear velocity vector
$\boldsymbol{v}(\boldsymbol{r})$	linear velocity vector at a point on ball surface at radius $\boldsymbol{r}$
$\boldsymbol{v}_c$	linear velocity vector of ball center
$\boldsymbol{v}_t$	linear velocity of ball at top contact
W	normal load on ball in scrub
ε	ball orbit angular velocity deficit
θ	angle defined in fig. 2

θ_{max} maximum angle included by scrub on spiral scrub track

μ coefficient of friction

Ω_o orbital angular velocity of ball center

Ω_p angular velocity of top plate

ω ball angular velocity vector

Experiment

Mechanics

The thrust bearing assembly is housed in a cubical stainless steel vacuum chamber. The bottom element, a circular stationary plate, is mounted on a ball joint that permits the two horizontal plates to achieve parallel alignment when the 12.7-mm- (0.5-in.-) diameter balls are in position and under the load (before any shaft rotation begins). The bottom plate is electrically isolated from ground to allow a determination of the electrical resistance from the lower plate to the upper plate through the six lubricated ball-plate contacts. This lower assembly is on a shaft supported by a ball bushing in vacuum. The shaft passes through a steel bellows and is attached (through a load cell in air) to a deadweight cantilever-type loading device that forces the shaft up, loading the bottom plate and balls against the top plate. The load was 445 N (100 lbf), yielding a mean Hertz stress of 1.39 GPa (0.2×10^6 psi) at the ball-plate contacts. This Hertz stress is typical for a preloaded instrument ball bearing.

The top plate is mounted on the shaft of a ferrofluidic-type rotary feedthrough on which the plate has a total indicated axial runout of approximately 0.013 mm (0.0005 in.). Rotation is produced by a synchronous gearmotor on the feedthrough shaft. A proximity sensor near the shaft of this feedthrough furnished a signal to a digital counter and a strip chart recorder. The pen mark on the recorder identifies the azimuthal position of the rotating top plate.

The guide plate is mounted on a piezoelectric force transducer (fig. 1) fixed to the chamber wall. The transducer signal gives the force on the ball as it is guided (forced) back to its starting position at a smaller radius on the repeated spiral track. This force will yield a friction coefficient. The signal from the transducer was displayed on the strip chart recorder.

The chamber was evacuated without bakeout by a turbomolecular pump to a base pressure of 1.1×10^{-7} Pa (8×10^{-10} torr), as determined by a cold cathode, Penning-type ionization gauge. A quadrupole residual gas analyzer (RGA) with a line of sight to the triboelements determines the composition of the residual gas in the test ambient and also the species evolved from the lubricant to the ambient by frictional processes. The RGA and the pressure gauge were chosen or modified to eliminate the electrons or ions that such devices can inject in the test environment. Electrons and ions can interact with radiation-sensitive materials such as fluorinated lubricants and can generate phenomena that could be mistaken for those of a truly tribological origin.

Materials

The three balls, two horizontal plates, and a guide plate are 440C steel, a material commonly used in instrument ball bearings. The three plates have a hardness R_c of 60 to 62. The bearing balls were obtained as commercial grade 25. The plates were polished to a mirror finish with diamond and alumina grit. The plates and balls were solvent-cleaned and then subjected to ultraviolet-ozone cleaning to remove carbonaceous surface contaminants. An analysis of the cleaned surfaces by x-ray photoelectron spectroscopy in our laboratory revealed a signal intensity due to adventitious surface carbon at about the level of the carbon signal due to the carbide phase in the steel.

The lubricant fluids, Dupont Krytox 16256 and Fomblin Z–25, are classified as perfluoropolyalkylethers and have a molecular weight of approximately 11 000 amu and an extremely low vapor pressure at room temperature. After pumpout and before starting rotation, no signals attributable to evaporating lubricants were detected by a residual gas analysis.

From a solution of the lubricant, a thin film was applied to each ball by dipcoating. A typical charge of lubricant on a ball was approximately 100 μg (2.2×10^{-7} lb), corresponding to an average film thickness of approximately 100 nm (4 μin.) for a lubricant specific gravity of 1.9. Although the lubricant film was not uniform over the surface of the ball, no effects of this nonuniformity were evident in the tribological data. Lubricant fluid was not applied to the plates, which acquire lubricant only by transfer from the balls.

Setup

The specimens had to be installed in a particular manner so that a coefficient of friction could be correctly obtained from the guide plate forces. This installation was based on the importance of the runout of the rotatable top plate. A dial indicator gauge fixed to the body of the chamber was used to identify the lowest point on the polished surface of the top plate and to place it the farthest from the guide plate (i.e., across the system axis). With the ball joint of the lower plate free, the balls were installed at symmetric positions, the load was applied to bring the specimens together, and the lower ball joint was secured. This procedure guaranteed that the two horizontal plates were parallel at an established top plate azimuthal position. This is also the azimuth at which the three balls shared the total load equally. The reason for this initial specimen configuration is discussed in the section Results and Discussion.

Analysis

The elements of ball motion described in the Introduction, roll, orbit, scrub, and spiral, provide a framework for discussing the tribometer. The first three elements form the basis of the analysis to determine the angular and linear velocity of the ball in and out of the scrub. The analysis will (1) describe the motion of the ball; (2) identify the locus of slip between the triboelements; (3) explain the significance of the force on the guide plate and the ability of the tribometer to determine the coefficient of friction; and (4) calculate the rate of energy loss in the system as a result of interfacial slip. The energy is lost to the lubricant and may be considered responsible for its breakup and degradation. The energy loss rate is discussed in the section Energetics.

The fourth element of ball motion, the spiral orbit, is not given the same quantitative analysis. Although the spiral is important for the operation of the tribometer because it produces the scrub (on which the measurement of the friction coefficient is based), friction and energy loss can be understood without a detailed discussion of the spiral source. The reader is referred to K.L. Johnson's studies of the spiral (refs. 6 to 8).

It is also recognized that many results of the analysis can be obtained as a limiting case of the general analysis available in texts on the kinematics of ball bearings (ref. 9). With their curved races, ball bearings require a more elaborate analysis than the simple and self-contained analysis of the sphere-on-flat geometry given herein. The objective is to describe the physics of motion in this system for those not familiar with the mathematics of ball bearing kinematics.

Kinematics

The balls and plates are initially considered to be rigid inelastic bodies; their elasticity is introduced later. The analysis is based on the requirement that the balls roll without slip at the contacts, which means that there is no relative linear velocity between the ball and plate at a contact. The reason for this requirement is that rolling friction is an order of magnitude smaller than sliding friction, even for the most favorable boundary-lubricated condition. The condition of roll without slip can be satisfied at all contacts in our system except for the contact of the ball on the top plate in the scrub region. This contact exhibits gross sliding. The motion outside the scrub is analyzed first.

Outside the scrub.—The relationship between the upper plate angular velocity and the orbital angular velocity of the ball center is obtained from the fundamental relation between the velocity of any point on the surface of the ball $\boldsymbol{v}(\boldsymbol{r})$ and the velocity of its center $\boldsymbol{v}_c$:

$$\boldsymbol{v}(\boldsymbol{r}) = \boldsymbol{v}_c + \boldsymbol{\omega}\times\boldsymbol{r} \tag{1}$$

where ω is the angular velocity vector of the ball and $\boldsymbol{r}$ is a radius vector from the ball center to any point on its surface. If $\boldsymbol{r}_b$ is the radius vector from the ball center to the top plate contact, the velocity of the ball at the top contact is

$$\boldsymbol{v}_t = \boldsymbol{v}_c + \boldsymbol{\omega}\times\boldsymbol{r}_b \tag{2}$$

If $\boldsymbol{V}$ is the velocity vector of the top plate at the point of contact, roll without slip requires that

$$\boldsymbol{V} = \boldsymbol{v}_c + \boldsymbol{\omega}\times\boldsymbol{r}_b \tag{3}$$

For the contact at the stationary bottom plate, $\boldsymbol{r} = -\boldsymbol{r}_b$ and roll without slip requires that

$$0 = \boldsymbol{v}_c - \boldsymbol{\omega}\times\boldsymbol{r}_b \tag{4}$$

Add equations (3) and (4) to obtain

$$\boldsymbol{v}_c = \frac{\boldsymbol{V}}{2} \tag{5}$$

This vector relation indicates that the ball is driven in the direction of the top plate velocity vector at the contact. The top plate rotates, driving the ball in a circular orbit, a consequence of roll without slip. Also, Ω_o, the orbital angular velocity of the ball center, and Ω_p, the top plate rotation rate, are related as

$$\Omega_o = \frac{\Omega_p}{2} \tag{6}$$

The ball center orbit rate is thus half the rotation rate of the top plate. This relationship is independent of the ball radius r_b and the radius to the contact from the shaft axis R. Thus, the circular motion of the ball center as well as its orbital rate are established as a consequence of roll without slip.

The angular velocity of the ball ω can now be determined. Subtract equation (3) from (4) to obtain

$$\boldsymbol{V} = 2\boldsymbol{\omega}\times\boldsymbol{r}_b \tag{7}$$

With the ball center orbiting clockwise in the $\boldsymbol{i}, \boldsymbol{j}$-plane, the specific coordinate system shown in figure 3 is now used: for the ball in the position shown, $\boldsymbol{r}_b = r_b\boldsymbol{k}$, $\boldsymbol{V} = |V|\boldsymbol{i}$, and $\boldsymbol{\omega} = \omega_i\boldsymbol{i} + \omega_j\boldsymbol{j} + \omega_k\boldsymbol{k}$. Substituting into equation (7) yields

$$|V|\boldsymbol{i} = 2r_b\left(-\omega_i\boldsymbol{j} + \omega_j\boldsymbol{i}\right) \tag{8}$$

where r_b is the ball radius.

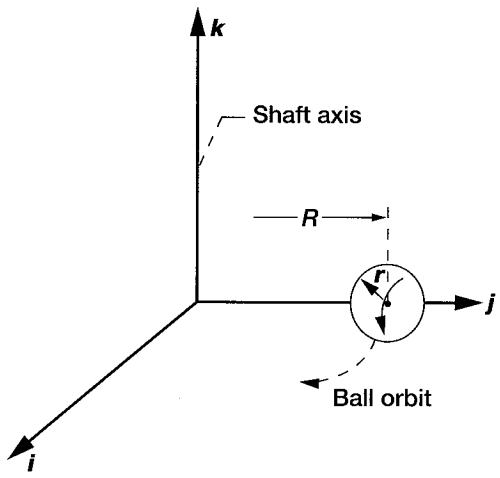

Figure 3.—Coordinate system used to analyze ball motion out of scrub region.

So that

$$\omega_i = 0 \tag{9a}$$

$$\omega_j = \frac{|V|}{2r_b} = \frac{\Omega_p R}{2r_b} \tag{9b}$$

Two of three components of ω have been determined. The relationship in equation (9b) is found in elementary texts and holds for unidirectional rolling as well as for the present circular orbit. Specifying the path of the ball determines ω_k, the third component of the angular velocity; in figure 2, consider the point on the ball on the j-axis that is farthest from the k-axis. For this point, $\boldsymbol{r} = r_b\boldsymbol{j}$. For the ball to orbit in a circle, the velocity of this point must be $\Omega_o(R + r_b)$ in the i-direction. Then, using equation (1),

$$\Omega_o(R+r_b)\boldsymbol{i} = \Omega_o R\boldsymbol{i} + \left(\omega_j\boldsymbol{j} + \omega_k\boldsymbol{k}\right)\times r_b\boldsymbol{j} \tag{10}$$

and therefore

$$\omega_k = -\Omega_o = -\frac{\Omega_p}{2} \tag{11}$$

This third component of angular velocity of the ball is also the orbital angular velocity of the ball center and is negative for the direction of rotation chosen herein. The complete angular velocity vector of the ball is

$$\boldsymbol{\omega} = \frac{\Omega_p R}{2r_b}\boldsymbol{j} - \frac{\Omega_p}{2}\boldsymbol{k} \tag{12}$$

This equation also implies that for a ball rolling without slip in a circular orbit, the locus of points of contact on the ball surface is a single great circle. The two means by which the rest of the ball surface and its lubricant can be brought into the contact are described later in this section.

An advantage of this formal derivation is that it makes explicit the vertical k-component of the ball angular velocity. The difference between this component and the angular velocity of the contacting plate is the relative angular velocity of the contact in a direction $\boldsymbol{k}$ normal to the plane of the contact. This relative angular velocity has been referred to as pivot and is discussed in the literature (ref. 10). The significance of pivot for elastic bodies with a nonzero area of contact is that it gives rise to sliding and frictionally induced energy loss within the contact area. If $\boldsymbol{P}_t$ is denoted as the relative plate-ball angular velocity of the top plate contact normal to the plane of contact,

$$\boldsymbol{P}_t = -\frac{\Omega_p}{2}\boldsymbol{k} \tag{13a}$$

and for the pivot of the bottom plate contact,

$$\boldsymbol{P}_b = +\frac{\Omega_p}{2}\boldsymbol{k} \tag{13b}$$

The magnitude of the sliding velocity at a radius r within the elastic circular contact region is $|\boldsymbol{P}|r$ and is the velocity that causes the energy loss for the rolling ball orbiting in a circle. Note that pivot and its associated energy loss are absent for a ball rolling in a straight line, even for elastic materials with a nonzero area of contact.

A numerical value of pivot-induced slip velocity in the tribometer can be obtained. The total load shared equally by the three balls yields a Hertz radius of 0.184 mm (7.2×10^{-3} in.); the 4-rpm shaft speed ($\Omega_p = 0.42$ rad/s) gives the maximum sliding velocity at the contact perimeter as 0.038 mm/s (1.5×10^{-3} in./s).

The kinematics of the retainerless thrust bearing and the angular contact bearing are related in that they both exhibit pivot (refs. 10 and 11). Note that the sum of the absolute pivots for the thrust bearing is Ω_p and that it has a contact angle $\pi/2$. According to published first-order kinematic formulas for angular contact ball bearings, the sum of the absolute pivots for any bearing in any rotational mode is its total speed times the sine of the contact angle. This relationship also holds for this thrust bearing and establishes its connection to those bearings with curved surfaces that also exhibit pivot.

Before the motion of the ball in the scrub is considered, some remarks on the spiral nature of the ball orbit are necessary. The spiral can be described (fig. 3) as the result of a nonzero i-component of the ball angular velocity vector ω. This component moves the locus of contact on the ball off the

great circle it would have if the orbit were a perfect circle and generated a contact spiral on the ball as it rolled and executed its spiral orbit on the bottom plate. It thus has the beneficial effect of continuously bringing new lubricant into the contacts and avoiding the continual stressing of only the lubricant in a single great circle on the ball. Another benefit this component provides is that it plays no role in interfacial slip and energy loss at the contacts because it is perpendicular to the angular velocity of the plates and therefore does not contribute to pivot as defined above. In view of these facts, the spiral is taken here simply as a characteristic of the motion that leads to the scrub. A discussion of the processes that lead to the spiral is found in references 6 to 8.

Inside the scrub.—Consider the ball moving at any point inside the scrub. The linear velocity $\boldsymbol{v}_c$ and the angular velocity $\boldsymbol{\omega}$ are sought subject to the requirement that there be roll without slip if possible. In figure 2, the spiral-scrub track is drawn as it appears on the bottom plate where the angle included by the scrub θ_{max} is 13.6°. The linear velocity of the ball center is $\boldsymbol{v}_c = |v_c(\theta)|\boldsymbol{i}$; the dependence on θ indicates the possibility that $|v_c|$ may vary throughout the scrub. Now let $\boldsymbol{\omega} = \omega_i \boldsymbol{i} + \omega_j \boldsymbol{j} + \omega_k \boldsymbol{k}$ and treat the contact with the stationary bottom plate where $\boldsymbol{r} = -r_b \boldsymbol{k}$. The velocity of the ball surface at this point must be zero for roll without slip, so

$$0 = |v_c(\theta)|\boldsymbol{i} + \boldsymbol{\omega} \times (-r_b \boldsymbol{k}) = \left[|v_c(\theta)| - r_b \omega_j\right]\boldsymbol{i} + r_b \omega_i \boldsymbol{j} \quad (14)$$

Therefore,

$$\omega_i = 0 \quad (15a)$$

$$\omega_j = \frac{|v_c(\theta)|}{r_b} \quad (15b)$$

and roll without slip on the bottom plate in the scrub is possible. Thus far, two components of $\boldsymbol{\omega}$ in the scrub have been determined. For the contact with the guide plate, $\boldsymbol{r} = r_b \boldsymbol{j}$ and roll without slip demands that the velocity of the ball surface at this contact be zero:

$$0 = |v_c(\theta)|\boldsymbol{i} + \left[\frac{|v_c(\theta)|}{r_b}\boldsymbol{j} + \omega_k \boldsymbol{k}\right] \times r_b \boldsymbol{j} = \left[|v_c(\theta)| - \omega_k r_b\right]\boldsymbol{i} \quad (16)$$

Therefore,

$$\omega_k = \frac{|v_c(\theta)|}{r_b} \quad (17)$$

The ball rolls without slip simultaneously on the bottom plate and on the guide plate. The complete angular velocity vector for the ball in the scrub is

$$\boldsymbol{\omega} = \frac{|v_c(\theta)|}{r_b}(\boldsymbol{j} + \boldsymbol{k}) \quad (18)$$

where $|v_c(\theta)|$ is now determined by considering the contact with the top plate $\boldsymbol{r} = r_b \boldsymbol{k}$. From figure 2, the velocity of the top plate at the contact is

$$\boldsymbol{V} = \frac{\Omega_p R_o}{\cos(\theta)}\left[\cos(\theta)\boldsymbol{i} + \sin(\theta)\boldsymbol{j}\right] = \Omega_p R_o\left[\boldsymbol{i} + \tan(\theta)\boldsymbol{j}\right] \quad (19)$$

The velocity of the ball surface at this contact is

$$\boldsymbol{v} = |v_c(\theta)|\boldsymbol{i} + \frac{|v_c(\theta)|}{r_b}(\boldsymbol{j} + \boldsymbol{k}) \times r_b \boldsymbol{k} = 2|v_c(\theta)|\boldsymbol{i} \quad (20)$$

The relative velocity at the contact is

$$\Delta \boldsymbol{V} \equiv \boldsymbol{V} - \boldsymbol{v} = \left[\Omega_p R_o - 2|v_c(\theta)|\right]\boldsymbol{i} + \Omega_p R_o \tan(\theta)\boldsymbol{j} \quad (21)$$

Roll without slip is possible for the $\boldsymbol{i}$-component of relative velocity if

$$|v_c(\theta)| = \frac{\Omega_p R_o}{2} \quad (22)$$

which determines the velocity of the ball center in the scrub. This velocity is independent of position in the scrub and is the same as the velocity outside the exit of the scrub (see eq. (5)). The complete angular velocity vector of the ball in the scrub can now be written as

$$\boldsymbol{\omega} = \frac{\Omega_p R_o}{2 r_b}(\boldsymbol{j} + \boldsymbol{k}) \quad (23)$$

Although the $\boldsymbol{i}$-component of relative velocity at the top plate contact can be zero, the $\boldsymbol{j}$-component is not zero. There is slip at this contact with a relative sliding velocity normal to the guide plate of

$$\Delta \boldsymbol{V} = \Omega_p R_o \tan(\theta)\boldsymbol{j} \quad (24)$$

This gross slip occurs only by the ball in the scrub sliding on the top plate; the direction of this slip is normal to the guide plate. Because slip generates a friction force in the direction of slip,

the force on the guide plate is normal to it and is the friction force required to slide the ball on the top plate. No radial friction force is developed on the bottom plate by the ball in the scrub because no gross slip is present there. The force on the guide plate is μW, where μ is the coefficient of friction for the ball sliding on the top plate with a velocity indicated in equation (24), and W is the normal load on the ball in the scrub. The identification of this force is the basis for the tribometer's capability to measure the coefficient of friction of the lubricated contacts. The sliding velocity is not constant but is a maximum 2.1 mm/s (0.084 in./s) at the entrance to the scrub and decreases to zero at the exit. The friction coefficient may depend on velocity and, therefore, the friction force, as indicated by the force transducer, may not be constant throughout the scrub.

The kinematic elements of pivot are now derived for the motion of the ball in the scrub. The angular velocity vector of equation (23) is used to show the pivot (ball-plate) for the three contacts. For the bottom plate contact,

$$\boldsymbol{P}_b = -\frac{\Omega_p R_o}{2r_b}\boldsymbol{k} \tag{25a}$$

the guide plate contact,

$$\boldsymbol{P}_g = -\frac{\Omega_p R_o}{2r_b}\boldsymbol{j} \tag{25b}$$

and the top plate contact,

$$\boldsymbol{P}_t = -\Omega_p\left(1+\frac{R_o}{2r_b}\right)\boldsymbol{k} \tag{25c}$$

These relative angular velocities cause interfacial slip in the elastic contact areas in the same way that the ball moving outside the scrub does. In the next section, the pivots are used to calculate the rate of energy loss in the lubricated contacts.

The second means by which fresh ball surface and lubricant are brought into contact is by the angular motion of the ball in the scrub. The $\boldsymbol{k}$-component of angular velocity, due to the ball rolling on the guide plate, rotates the ball off the spiral of contact it had upon entering the scrub and thus generates new spirals of contact each time the ball passes through the scrub region. The first means of bringing fresh ball surface and lubricant into the contact was based on the spiral character of the ball orbit. Both means allow the entire ball surface to eventually be brought into contact and all the lubricant film on its surface to be stressed. Another aspect of the angular motion, when the ball slides on the top plate, is that the same spot on the ball is not always in contact, even within a given pass of the ball through the scrub. The ball's angular velocity brings new surface into the sliding contact during the traverse through the scrub. This motion is different from that of the ball-on-flat sliding configurations where the same spot on the ball is continuously being slid upon, generating a flat wear spot. All areas of the ball in the tribometer are expected to be subjected eventually to the sliding in the scrub (given enough traverses), and thus no specific regions of wear or distress should appear on the ball, even after thousands of top plate revolutions. In fact, thousands of revolutions tend to remove any specific distress on the ball.

Energetics

Energy is dissipated in this system as a result of sliding within the pivoting contacts and, for a ball in the scrub, at the gross sliding contact at the top plate. Herein, the rate of energy dissipation is termed "severity" and is denoted by S. Severity is considered because lubricant fragments are released to the ambient by frictional processes. If it is assumed that the energy loss in these contacts is related to lubricant degradation, it is reasonable to assume that the energy loss rate is directly proportional to the rate at which fragments of degraded lubricant are released to the ambient and are detected by the RGA. The intensity of the fragment emission increases when the ball passes through the scrub. This motivates one to calculate the ratio of the severity for the ball passing through the scrub to the severity for all three balls moving outside the scrub. A comparison of calculated severities with experimental RGA intensities provides support for the present analysis of ball motion.

Severity can be calculated from the product of force and velocity; hence, the severity for pivot-induced sliding within the elastic contact areas can be written as

$$S = \int \boldsymbol{F}\cdot\boldsymbol{v}\,\mathrm{d}A \tag{26}$$

where $\boldsymbol{F}$ is the sliding force per unit area, $\boldsymbol{v}$ is the velocity, and the integration is over the circular area of contact A. The force is always in the direction of velocity in a frictional contact and is given by the product of the coefficient of friction μ and the local pressure at any radius from the center of the contact r:

$$\boldsymbol{F} = \frac{3\mu W}{2\pi r_H^2}\sqrt{\left(1-\frac{r^2}{r_H^2}\right)} \tag{27}$$

where W is the load normal to the interface and r_H is the radius of the elastic (Hertzian) contact for load W. As pointed out in a previous section (*Outside the scrub*), the velocity is $|\boldsymbol{P}|r$, where $|\boldsymbol{P}|$ is the magnitude of the pivot. Substituting these expressions and performing the integration gives, for a pivoting contact,

$$S = \frac{3\pi}{16}\mu|\boldsymbol{P}|Wr_H \tag{28}$$

With $|\boldsymbol{P}| = \Omega_p/2$, the system severity for three balls moving outside the scrub is

$$S_{\text{out}} = \frac{3\pi}{32}\mu\Omega_p W r_H \cdot 6 \tag{29}$$

where W is the load per ball and the factor of 6 accounts for two contacts on each of the three balls.

The severity for the ball in the scrub sliding on the top plate is obtained from equation (24) as

$$S = \mu W|\Delta V| = \mu W\Omega_p R_o \tan(\theta) \tag{30}$$

where the friction coefficient is assumed to be the same for gross sliding and pivot sliding. The system severity for one ball in the scrub and two balls out of the scrub is

$$S_{\text{in}} = \frac{3\pi}{32}\mu\Omega_p W r_H \sum_{n=1}^{5} A_n \tag{31}$$

where, for two contacts for each of two balls pivoting outside the scrub,

$$A_1 = 4$$

In contact with the bottom plate for a ball pivoting in the scrub,

$$A_2 = \frac{R_o}{r_b}$$

In contact with the guide plate for a ball pivoting in the scrub,

$$A_3 = \mu^{4/3}\frac{R_o}{r_b}$$

In contact with the top plate for a ball pivoting in the scrub,

$$A_4 = 2 + \frac{R_o}{r_b}$$

For a ball in the scrub sliding on the top plate,

$$A_5 = \frac{32}{3\pi}\frac{R_o}{r_H}\tan(\theta)$$

It has been assumed herein that the friction coefficient is not a function of velocity. Also, note that the severity at the top plate contact in the scrub was calculated with separate severities for pivot-induced sliding and gross sliding. This procedure is not strictly correct in that the vector sum of these velocities should have been used in a single severity integral; however, this separation allowed the different contributions to the total severity to be clearly displayed. An exact calculation changes by less than 2 percent the numerical results to be presented next.

The severities can be evaluated to provide absolute numerical energy dissipation rates. However, it is more appropriate to evaluate the system severity during the passage of a ball through the scrub relative to the system severity for all balls moving outside the scrub. The form in which the system severities are given (eqs. (29) and (31)) facilitates the evaluation of the relative severity $S_{\text{in}}/S_{\text{out}}$. This relative system severity can be compared with the signal intensity of a released lubricant fragment in the RGA as a ball traverses the scrub. The values for R_o, r_b, r_H, and $\theta_{\max}$ have already been given; next, a value of μ is chosen to be 0.4. The relative severity (fig. 4) immediately increases by a factor of 17.6 at the entrance to the scrub and then decreases linearly to 2.2 at the exit. This behavior is entirely attributed to the variation of the gross sliding velocity of the ball on the top plate. The numerical values indicated here are very insensitive to the particular value chosen for the friction coefficient, which, in this calculated severity profile, is assumed to be constant throughout the scrub. A comparison of this calculated behavior with experiment is made in the next section.

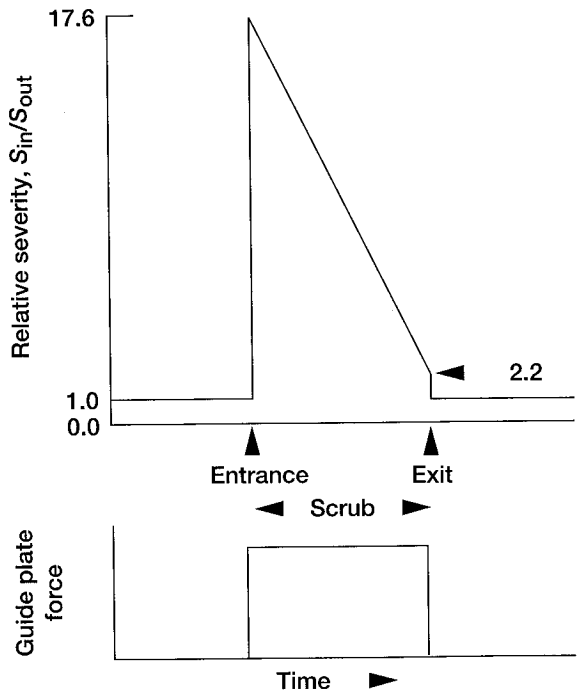

Figure 4.—Calculated relative severity S_{in}/S_{out} and contact force on guide plate as ball passes through scrub region.

Results and Discussion

The results are presented in two parts. The first comprises experimental observations that relate specifically to and support the analysis. The second deals with experimental observations that relate to the tribometer's operation to provide information about the friction in the boundary lubrication regime.

Validation of Analysis

Five observations directly support the analysis. First, the ball's orbit is close to being circular, as predicted by equation (5), and is a consequence of roll without slip. Second, a related prediction from equation (6) is that the ball orbit angular velocity is half that of the top plate. This prediction was tested by counting the number of orbits of a given ball for a given number of top plate revolutions, which should be a ratio of 1:2. The counting was facilitated by the signals from the shaft revolution counter and the force transducer, both of which appeared on a strip chart recorder during operation. For a given ball, the ratio of the number of ball contacts with the guide plate to the number of top plate revolutions was maintained at 1:2 for thousands of top plate revolutions. The prediction of equation (6) was thus well supported. Eventually, however, the number of ball contacts fell behind the predicted value because the ball orbit rate was slightly less than half that of the top plate. This "orbital velocity deficit," although a small fraction of the ball orbit velocity, can strongly affect the time dependence of the force on the guide plate, as discussed later in Characteristics of a Test.

The third observation relates to the appearance of the specimens. An examination of a ball that orbited thousands of times revealed tracks from the remaining lubricant. When the lubricant was removed with a solvent, the ball was in an original, pristine condition. At the end of the test, the same condition was evident even for a ball examined after a few revolutions when the lubricant had transferred off (as indicated by the great increase in friction). The absence of a preferentially worn, banded, or exercised region on a ball is in accordance with the analysis because the spiral nature of the contact locus on the ball and the rolling of the ball against the guide plate bring fresh surface and new lubricant into the contact. No particular region of the ball surface was expected to receive preferential treatment and none was observed. The removal of degraded and/or excess lubricant on the plates revealed only faint scratches and no significant wear. Thus, the flatness of the plates and sphericity of the balls appeared to be maintained, justifying the use of an elastic sphere-on-flat analysis of the contacts throughout the operation. This analysis may be contrasted to that performed with a sphere-on-flat sliding geometry in which the development of wear scars soon precludes conducting a simple elastic analysis of the contact stress.

A fourth observation relates to the analysis of the ball moving in the scrub. This analysis indicated that the ball slides on the top plate, producing a frictional sliding force there and not on the bottom plate. This conclusion was tested by operating with no lubricant applied to the specimens. The guide plate force was high and operation was stopped after only a few contacts. Examination revealed that a short sector of the top plate track exhibited severe metal distortion and flow associated with the galling of clean sliding metal, as shown in the photomicrograph of figure 5. This short sector was generated as the ball passed through the scrub. The metal distortion is evidence of large frictional forces on the top plate; however, neither the bottom plate nor the guide plate exhibited such distorted metal. This contrast in the damage on the plates with the clean contacts is taken as confirmation that the measured friction force results from a ball sliding only on the top plate and not on the bottom plate or the guide plate.

The fifth observation concerns the energy dissipation rate (severity) in the system (fig. 4). As noted in the analysis that led to this figure, the severity should be directly proportional to the intensity of an RGA signal generated by the fragment of a decomposing lubricant molecule, Fomblin Z–25 in the present case. The intensity of the fragment (m/e = 44 (CO_2^+)) in the RGA and the signal from the force transducer on the strip chart recorder are shown in figure 6. Note that the force is not constant throughout the scrub but decreases gradually before the ball leaves the scrub. This time-dependent force was observed for all lubricants. Its shape is not constant and may be attributed to a dependence on sliding velocity or another aspect of motion not taken into account in this analysis. In any case, this nonconstant force means that the conditions for which the severity profile (fig. 4) were calculated are not completely satisfied. However, there is enough of a "flat top" to compare the experimental RGA intensity (fig. 6) with the severity profile

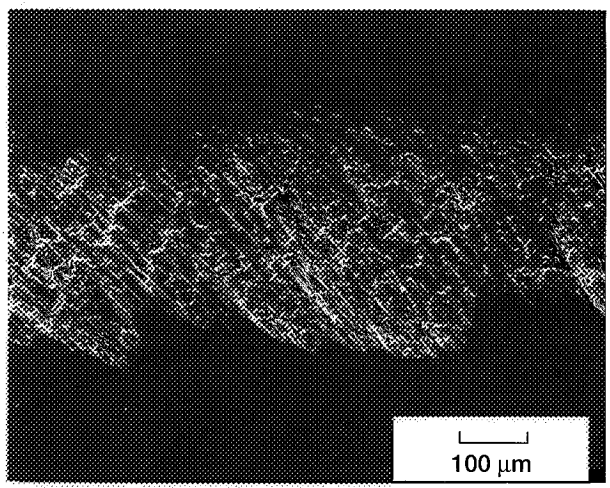

Figure 5.—Electron micrograph of contact region on top plate after test without lubricant.

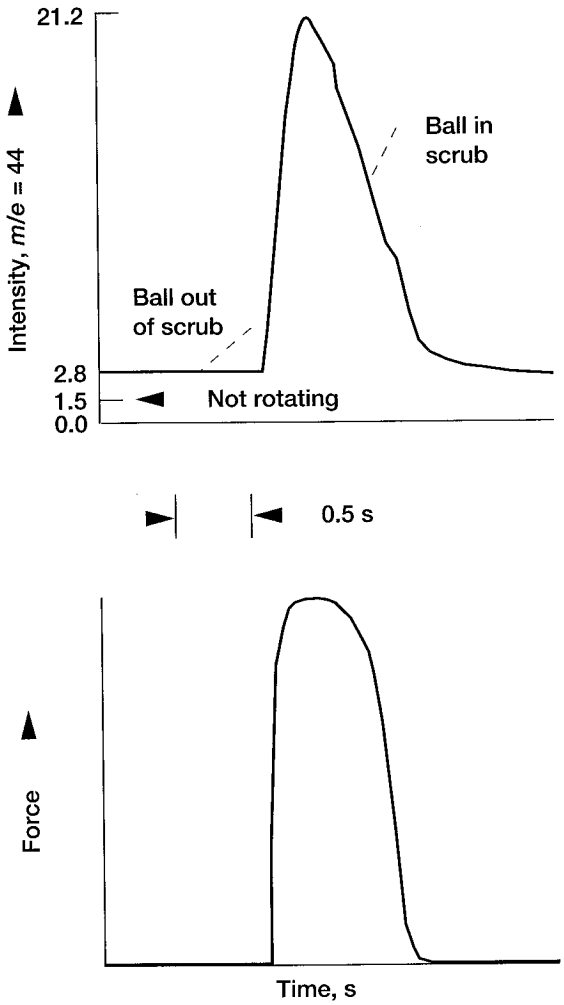

Figure 6.—Upper trace shows experimental intensity of residual gas analyzer signal for m/e = 44 (CO_2^+); lower trace shows contact force on guide plate as ball lubricated with Fomblin Z-25 passes through scrub region.

(fig. 4). The characteristic of the experimental intensity shape is an abrupt increase to a maximum at the entrance to the scrub and then a linear decrease to the initial value at the exit. This shape has been found for all the fragments of lubricants evaluated and thus appears to be characteristic of the kinematics of the system and not to be related to a specific fragment or lubricant. This observation is in accordance with the linear decrease shown in figure 4. A more quantitative comparison was made by noting that the ratio of the maximum intensity for a ball in the scrub to the intensity for all three balls outside the scrub is 15.2, close to the predicted value of 17.6. The agreement of these aspects of calculated severity and observed intensity in the RGA provides support for the analysis presented in the section on contact stresses and energetics. However, making this comparison was complicated because each ball did not exhibit the same friction force each time it passed through the scrub. This aspect of the instrument will be discussed more fully in the next section on the time dependence of the friction.

Characteristics of a Test

Whether tribological tests are simple linear sliding pin-on-disk tests or full-fledged bearing tests, they exhibit three stages of development. The first is the initial, or run-in, stage during which the tribological specimens or lubricants establish some equilibrium configuration. This configuration leads to the steady state, or equilibrium, stage in which the friction and other conditions of the system such as temperature are constant with time. After sufficient time elapses, failure, the third stage, occurs and the friction suddenly increases. This stage is usually considered the point at which the lubricant failed or was used up, or the solid tribological elements wore to an unacceptable degree. A test using this rolling contact tribometer also exhibits three stages, which are described next in this section.

The initial stage here was associated with the outward spiral of the rolling balls from their initial radii to radii at which they contacted the guide plate and established their equilibrium track. During these initial spiral orbits, the balls transferred some of their lubricant to the plates. The amount transferred was not controlled or known and was no longer available for the rest of the test. Therefore, the amount of lubricant that was actually available for the steady state stage was unknown and is an uncontrolled variable in the operation of the tribometer. However, experience thus far revealed that this variable was not a major factor because correlations with the initial lubricant charge and tribological quantities such as friction and test lifetime could still be established. The initial stage concluded with the balls contacting the guide plate, typically after less than 20 shaft revolutions. No conventional run-in was observed in the tribometer because the guide plate forces for the first few contacts were not different from those seen later in the steady state stage; hence, the steady state stage appeared to be established with the first contact of the guide plate.

The steady state stage is considered in terms of the guide plate forces recorded on a strip chart as the balls were driven through the scrub by the rotating upper plate. These data appear in figure 7 for three successive balls and in figure 8 for approximately 650 revolutions of the upper plate. Figure 7 indicates that successive ball passes produced different guide plate forces. The force due to a particular ball changes systematically, as shown in figure 8. Over 650 top plate revolutions, the force due to ball A decreased, the force due to ball B attained a maximum value and then decreased, and the force due to ball C increased. Note the regularity exhibited by the friction force data in figure 8. In the boundary regime, data are frequently noisy and difficult to reproduce. In contrast, these data are regular and noise free within an overall oscillatory behavior,

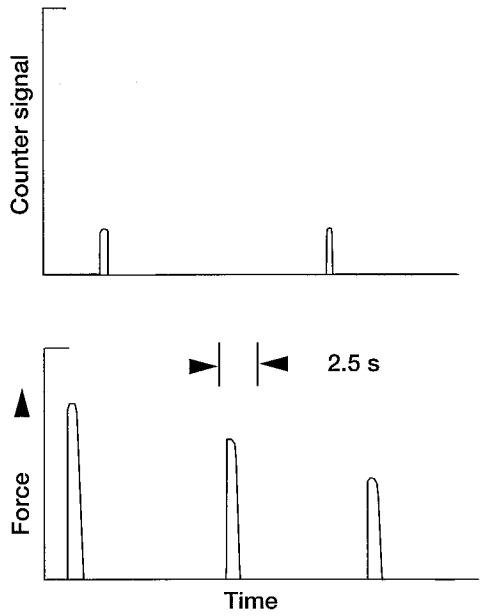

Figure 7.—Contact forces on guide plate as result of three balls successively passing through scrub region. Upper trace is from shaft revolution counter and indicates azimuth of top plate. Lower trace is contact force on guide plate as result of each of three balls passing through scrub.

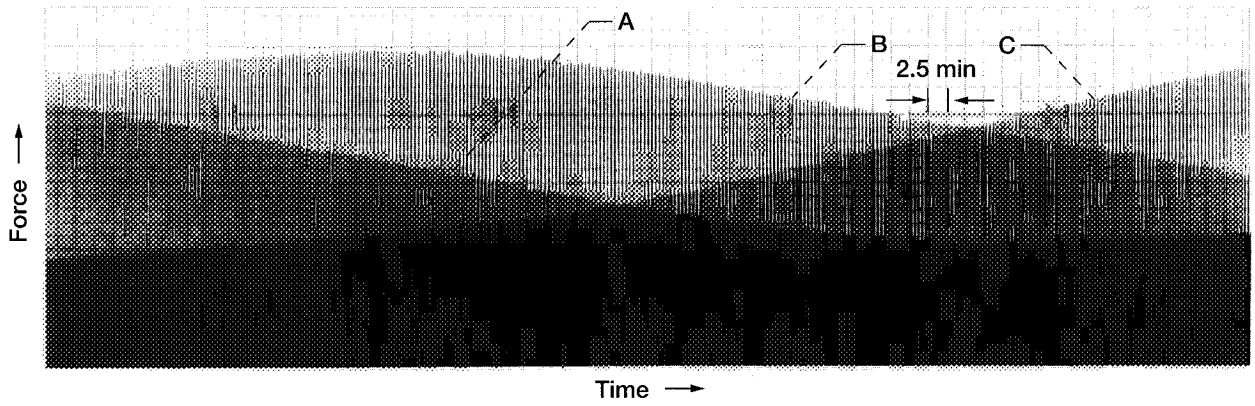

Figure 8.—Contact forces on guide plate as result of balls passing through scrub region for 650 revolutions of top plate. Note that contact force due to each ball (A,B,C) changes for successive contacts by that ball. Lubricant, Krytox 16256.

which is attributed to the continuous feeding of fresh surface into the frictional contact at the top plate and the refreshing of its lubricant supply. These lubricant supply mechanisms were discussed at the end of the Kinematics section.

The change in the guide force of a particular ball is oscillatory (fig. 9) for a test with Fomblin Z–25. This behavior was observed with all liquid lubricants and was a characteristic of this tribometer. Note that the maximum and minimum forces due to each ball are the same for all three balls (fig. 9) and that these extrema values do not change with thousands of top plate revolutions; however, the values do depend on the particular lubricant and its initial thickness. The steady state stage herein is defined as the constancy of these force oscillations and not as the constancy of the force due to a particular ball for many top plate revolutions. If the forces were constant and the same for each ball, it would be possible to assign each ball a normal load

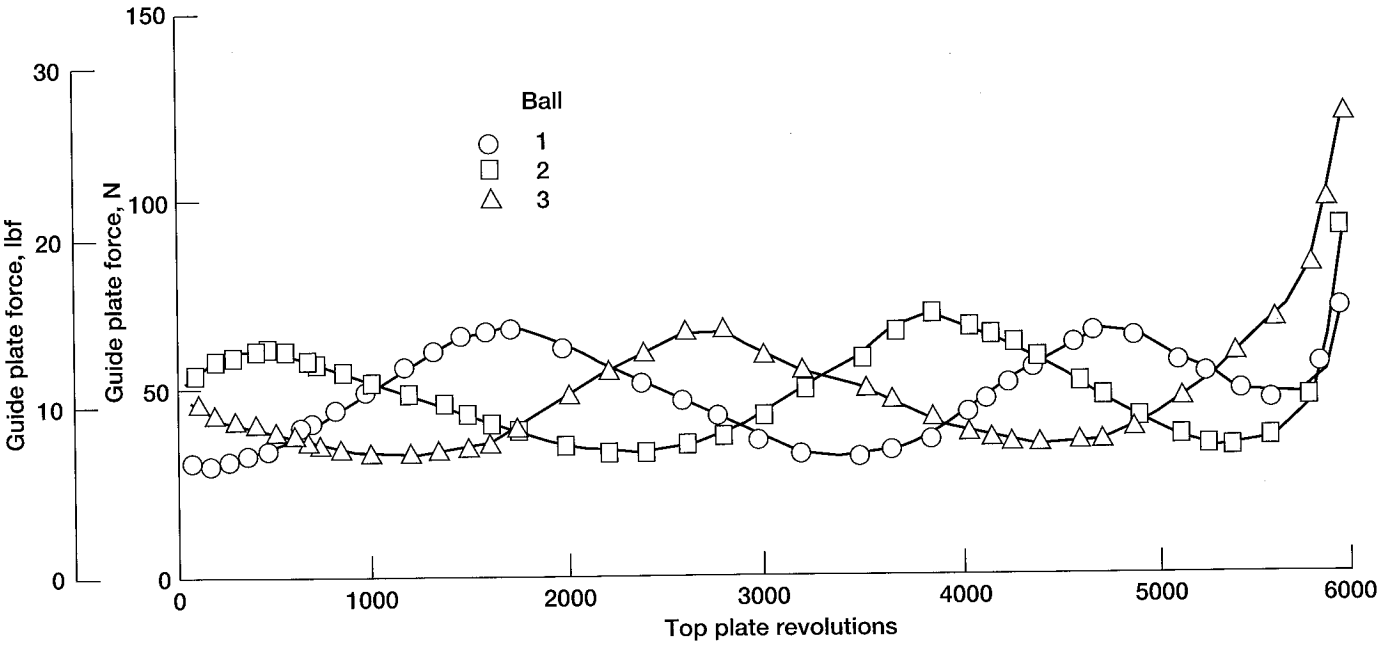

Figure 9.—Contact force on guide plate for complete test with Fomblin Z-25. The force due to each ball is oscillatory as a function of top plate revolutions. Note abrupt increase at ≅ 5500 revolutions.

of one-third the total load and obtain a friction coefficient as the guide plate force divided by the normal load. The systematic behavior actually observed is not so simple and is now explained.

The explanation of the friction data is based on two phenomena, the first of which is the effect of axial runout of the top plate. The runout of the top plate affects the normal load imposed on a ball. Recall that the specimens were initially installed with the plates parallel, and the lowest point on the top plate was placed across the shaft from the guide plate. An exaggerated view of this configuration is shown in figure 10. With the top plate at this initial azimuth, each ball receives the same normal load of one-third the total load. For any other azimuthal position of the top plate, the spacing between the plates at the scrub position is reduced to a value less than that for the initial setup because of the plate runout. A ball in the scrub is squeezed and subjected to a normal load higher than one-third the total load. As a ball orbits and passes through the scrub, it is contacted by a different azimuth of the top plate and thus receives a different normal load and develops different friction forces on the guide plate as it slides on the top plate. This configuration accounts for the different guide plate forces generated by successive balls passing through the scrub. Only if a ball passes through the scrub when the azimuth of the top plate is at its original setup position does the ball receive the lowest normal load of one-third the total load and thus develop its lowest friction sliding on the top plate. Therefore, the procedure is to seek the lowest friction force of a given ball on the strip chart, assign a normal load of one-third the total load, and calculate a friction coefficient. The coefficient must be the same for all balls because figure 9 indicates that the extrema are the same for all balls. Thus, in figure 9, the minimum guide plate force of 32 N (7.1 lbf) divided by 147 N (33.3 lbf) yields a friction coefficient of 0.21 for this test.

The second basis for the explanation of the friction data is an implication drawn from the presence of the oscillations in figure 9. They should not be present because the kinematic ratio of 1:2 of the top plate angular velocity to the ball orbit angular velocity brings the ball into contact with the same point of the top plate each time the ball is in the scrub. This behavior would produce the same normal load and friction force for each pass through the scrub instead of producing the observed oscillatory behavior. This behavior can be explained if the ball orbit angular velocity were less than the kinematically predicted value of half the angular velocity of the top plate. Then, a given ball would be contacted by successively different points on the top plate each time it passed through the scrub, and eventually all points on the top plate would be contacted by the ball as it passed through the scrub. The full range of normal loads due to top plate runout would then be imposed on a ball in the scrub, and the oscillatory behavior in figure 9 would be exhibited.

That the balls are actually orbiting at an angular velocity slightly less than the kinematically predicted value may be demonstrated and a value for the difference obtained. The signal on the strip chart from the shaft counter is used as a fiducial mark with which the arrival time of a ball in the scrub can be compared. The difference in these times changes linearly with successive top plate revolutions, with the ball arriving in the scrub later and later relative to the top plate azimuth. The angular velocity deficit of the ball orbit relative to the

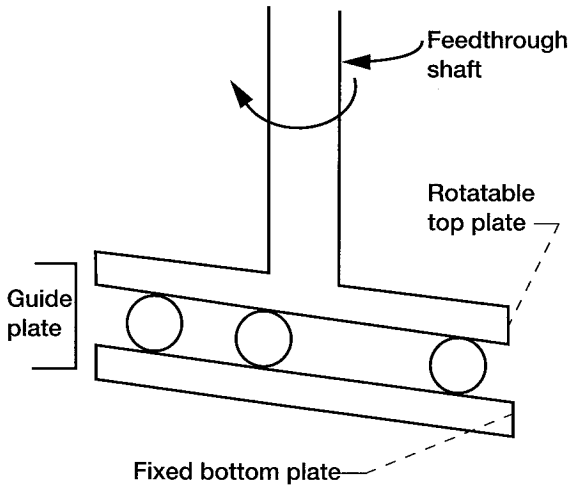

Figure 10.—Configuration of balls and plates as installed, indicating that lowest point of upper plate is initially placed opposite guide plate. Bottom plate is thus tilted with its highest point permanently at guide plate.

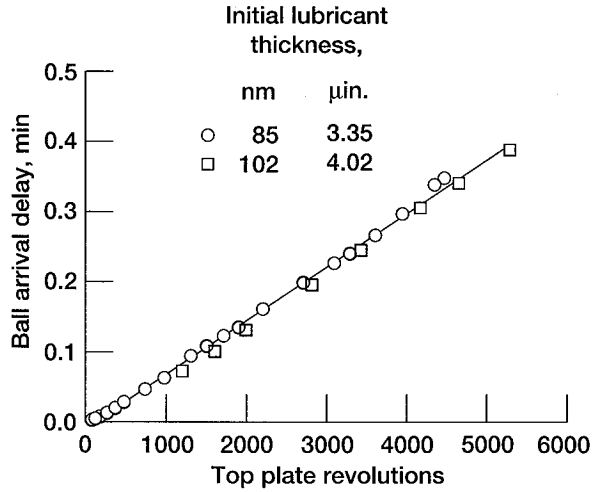

Figure 11.—Difference in arrival time for top plate and ball in scrub versus top plate revolutions for two tests with Fomblin Z-25.

kinematically determined value is denoted as ε and is defined through equation (6) as

$$\Omega_o = \frac{\Omega_p}{2} - \varepsilon \tag{32}$$

A plot of the arrival time difference versus top plate revolutions should be linear with a slope given approximately by

$$\text{Slope} = \frac{2\varepsilon}{\Omega_p^2} \tag{33}$$

The arrival time difference for two tests is shown in figure 11; one test furnished the data shown in figure 9 and the other test had a larger lubricant charge, a lower friction, and a longer steady state stage. Both tests had the same oscillation period. The data from the two tests are indistinguishable, demonstrating the highly reproducible deficit phenomenon. The plot shows that the ball does arrive in the scrub later and later relative to the top plate azimuth, verifying the existence of the ball orbit angular velocity deficit. The slope of this linear plot is 7.70×10^{-5} min/revolution, which yields a value of $\varepsilon = 6.16\times10^{-4}$ rpm from equation (33). Although this velocity deficit is a small fraction of the nominal ball orbit rate of 2 rpm, it is responsible for the dramatic oscillations of the friction force data shown in figure 9. The deficit is also responsible for the number of ball orbits falling behind half the number of top plate revolutions (which was mentioned in the section Validation of the Analysis). The direct connection of the velocity deficit ε and the oscillation period n_{osc} is given by

$$n_{osc} = \frac{\Omega_p}{2\varepsilon} \tag{34}$$

The value of ε found here gives an n_{osc} of 3247 revolutions, which, by inspection of figure 9, is shown to be close to the observed period. Therefore, the unusual appearance of the friction force data obtained with the tribometer can be understood as a consequence of the runout of the top plate and as a deficit in the orbital angular velocity of the ball relative to the orbital angular velocity demanded by the kinematics of the system.

The presence of runout and the attendant varying load on the balls complicates the aforementioned comparison of the calculated severity and the RGA signal intensity. The calculation assumed a constant load on the balls in their orbit and in the scrub. This assumption is not completely satisfied in the tribometer. A more complete calculation of the severity would have to include the effects due to runout. Nevertheless, the agreement with the calculated severity and the observed RGA intensity is still close enough to give credence to the general approach.

To summarize the steady state stage, the guide force data are characterized by two features. The first is that different values of the guide force were obtained for the three balls because the runout of the top plate imposed different loads on a ball in the scrub. Only the lowest value of the guide force can be associated with a known load of one-third the total load. The second feature is the oscillatory nature of the guide force on a given ball. The oscillation resulted from a velocity deficit (the orbital angular velocity of the ball being slightly less than the kinematically predicted value of half the angular velocity of the top plate), which was quantitatively determined and was consistent with the observed oscillation period. In fact, it is fortunate that

the velocity deficit is present in the system because it allows the full range of guide forces to be displayed. If it were not present, the lowest possible value of the guide force could not be attained and the friction coefficient could not be determined.

Failure, the third stage and the end of running, occurs with one of two conditions. The first is that the friction suddenly increases, indicating the absence of lubrication (the case shown in fig. 9). The increase in friction may be attributed to the transfer and displacement of lubricant to the side of the tracks where it is no longer available to the contacts. Some lubricant that is soluble and presumably unaltered by the test has been found adjacent to the track in posttest examinations. Physical properties such as viscosity and spreadability evidently determine the lubricant's ability to be displaced and to flow back into the track for further use. Whether this displacement is the dominant factor bringing the test to an end cannot easily be determined. A comparison of run times for different lubricants would have to take into account the properties that might allow one lubricant to remain in the track longer than the others before it was moved aside. Displaceability or spreadability is also a factor in other tribotests when the supply of lubricant is limited.

The friction also increases when the lubricant is used up. Volatilization by tribochemical degradation, for example, is present in the rolling element system. Degradation was demonstrated by an increase in the fragment of a decomposing molecule (m/e = 44) in the RGA during rotation. Thermal volatilization is absent here because of the low velocities and an attendant low temperature rise. In addition to volatilizing away, the lubricant may also transform under tribological stress to a solid material, sometimes called a friction polymer. A photomicrograph of the track after a test with Fomblin Z–25 (fig. 12) shows a central discolored region of the track that is insoluble in the same fluids which dissolve the lubricant, thus earning it the name friction polymer. It is not clear if this polymer is itself a lubricant or if it contributes to higher friction.

A number of mechanisms can cause a rise in friction. A detailed examination of the specimens after the test and comparisons of lubricants are necessary before conclusions can be drawn as to which mechanism may be dominant. Of course, the mechanism of failure may also be difficult to determine in the evaluation of lubricants in full-scale bearing tests.

The second condition that terminates a test is the loss of the balls' initially symmetric azimuthal positions with respect to each other and their beginning to touch and rub one another. Because this rubbing is not present in tests that terminate from high friction, a comparison of such tests is not appropriate. Also, the ball-to-ball rubbing is not included in the Analysis section because the reason for the development of azimuthal asymmetry is not known and requires further study. In any case, before the asymmetry develops, it should be possible to conclude a test with high friction by reducing the initial charge of lubricant on the balls.

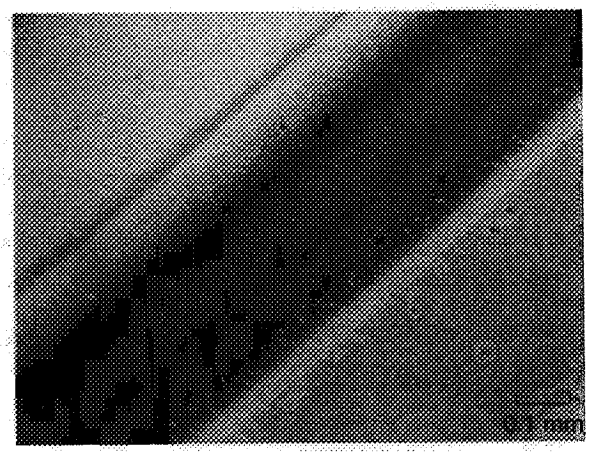

Figure 12.—Optical micrograph of track on bottom plate after completion of test with Fomblin Z–25.

Concluding Remarks

A new rolling contact tribometer for the evaluation of liquid lubricants in a vacuum was described and can be used as a test bed to exercise liquid lubricants in the operation of ball bearings. It allows a quantitative characterization of the contact conditions to which the lubricant is subjected and a way to easily examine the degraded lubricant using surface and thin-film analysis techniques.

The analysis of the contact identified two loci of slip: the first is the pivot slip due to the relative angular velocity normal to the ball's plane of contact as it rolls on the plates. This type of slip is present in angular contact ball bearings and provides the most direct correspondence of this simpler system's kinematics with those of the typical ball bearing. The other type of slip, gross sliding, occurs between the ball and the rotating upper plate when the ball is in the scrub. It may be likened to the sliding of a ball against the pocket of a retainer in the angular contact ball bearing. In fact, the guide plate *is* a retainer in that it keeps the balls in their radial position and from falling out. Also, the unknown sliding of a ball against a retainer pocket was exchanged herein for the known sliding of a ball against the upper plate when the ball is in the scrub.

Two phenomena of ball motion, however, are not well understood. The first is the outward spiral of the ball orbit, the origins of which are of interest because it is responsible for the presence of the scrub which affords the opportunity to measure the friction coefficient in this system. The second phenomenon is the ball orbit angular velocity deficit. It is partly responsible for the oscillatory appearance of the guide force data; it appears to be related to liquid lubricants because it was not found when the plates were lubricated with the solid lubricant molybdenum disulfide; its value is different for different liquid lubricants. Whether it is generated in or out of the scrub is not known. The deficit is not important to the system kinematics because it is

only a small fraction of the ball orbit angular velocity; rather, it is important in our quest for knowledge about liquid-lubricated rolling friction, which will be addressed in future reports.

The emphasis in this report was on the description, operating mode, contact conditions, and energy loss at the ball-plate contacts of the tribometer. Future publications will address the tribological features and chemical evolution of liquid lubricants used in this instrument. The tribological features of interest are the coefficient of friction and the lifetime of a given amount of liquid lubricant. Lifetime is not so clearly a property because other factors contribute to the lifetime of a test. The chemical evolution of the lubricant will be studied with the residual gas analyzer during a test. After the test, a variety of surface and thin-film analytical techniques (x-ray photoelectron spectroscopy (XPS) and infrared and Raman microspectroscopy) will be used to characterize the entity into which the lubricant evolves.

The engineering community will ultimately benefit from tests run with liquid lubricants in this tribometer because researchers will be able to choose different candidate lubricants for a particular application. The apparatus may also contribute to the knowledge of basic materials science because it generates friction polymers in a well-understood and controlled system and provides a way to systematically study these poorly understood materials.

Lewis Research Center
National Aeronautics and Space Administration
Cleveland, Ohio, August 23, 1996

References

1. Kingsbury, E.: Tribology in Slow Rolling Bearings. Mater. Res. Soc. Symp. Proc., vol. 140, 1989, pp. 437–442.
2. Kingsbury, E.: Kinematics of an Elastic Sphere Rolling on a Plane and Between Two Planes. J. Tribol., vol. 115, no. 3, July 1993, pp. 476–480.
3. Kalogeras, C.G., et al.: The Use of Screening Tests in Spacecraft Lubricant Evaluation. TR–93(3965)–6, The Aerospace Corp., Technology Operations, El Segundo, CA, Oct. 1993.
4. Lovell, M.R.; Khonsari M.M.; and Marangoni, R.D.: Low-Speed Friction Torque on Balls Undergoing Rolling Motion. Tibol. Trans. vol. 36, no. 2, April 1993, pp. 290–296.
5. Todd, M.K.J.; and Johnson, K.L.: A Model for Coulomb Torque Hysteresis in Ball Bearings. Int. J. Mech. Sci., vol. 29, no. 5, pp. 339–354, 1987.
6. Johnson, K.L.: The Effect of a Tangential Contact Force Upon the Rolling Motion of an Elastic Sphere on a Plane. J. Applied Mech., vol. 25, 1958, pp. 339–346.
7. Johnson, K.L.: The Effect of Spin Upon the Rolling Motion of an Elastic Sphere on a Plane. J. Applied Mech., vol. 25, 1958, pp. 332–338.
8. Johnson, K.L.: The Influence of Elastic Deformation Upon the Motion of a Ball Rolling Between Two Surfaces. Proc. Instn. Mech. Engrs., vol. 173, no. 34, 1959, pp. 795–810.
9. Hamrock, B.J.; and Dowson, D.: Ball Bearing Lubrication: The Elastohydrodynamics of Elliptical Contacts. John Wiley and Sons, New York, 1981.
10. Kingsbury, E.: Pivoting and Slip in an Angular Contact Bearing. ASLE Trans., vol. 27, July 1984, pp. 259–262.
11. Kingsbury, E.: First Order Ball Bearing Kinematics. ASLE Trans., vol. 28, April 1985, pp. 239–243.

REPORT DOCUMENTATION PAGE

Form Approved
OMB No. 0704-0188

1. AGENCY USE ONLY (*Leave blank*)	2. REPORT DATE	3. REPORT TYPE AND DATES COVERED
	October 1996	Technical Paper

4. TITLE AND SUBTITLE

A Rolling Element Tribometer for the Study of Liquid Lubricants in Vacuum

5. FUNDING NUMBERS

WU–297–40–01

6. AUTHOR(S)

Stephen V. Pepper, Edward Kingsbury, and Ben T. Ebihara

7. PERFORMING ORGANIZATION NAME(S) AND ADDRESS(ES)

National Aeronautics and Space Administration
Lewis Research Center
Cleveland, Ohio 44135–3191

8. PERFORMING ORGANIZATION REPORT NUMBER

E–10309

9. SPONSORING/MONITORING AGENCY NAME(S) AND ADDRESS(ES)

National Aeronautics and Space Administration
Washington, D.C. 20546–0001

10. SPONSORING/MONITORING AGENCY REPORT NUMBER

NASA TP–3629

11. SUPPLEMENTARY NOTES

Stephen V. Pepper, and Ben T. Ebihara, NASA Lewis Research Center; Edward Kingsbury, Interesting Rolling Contact, Walpole, Massachusetts 02081. Responsible person, Stephen V. Pepper, organization code 5140, (216) 433–6061.

12a. DISTRIBUTION/AVAILABILITY STATEMENT

Unclassified - Unlimited
Subject Category 27

This publication is available from the NASA Center for AeroSpace Information, (301) 621–0390.

12b. DISTRIBUTION CODE

13. ABSTRACT ***(Maximum 200 words)***

A tribometer for the evaluation of liquid lubricants in vacuum is described. This tribometer is essentially a thrust bearing with three balls and flat races having contact stresses and ball motions similar to those in an angular contact ball bearing operating in the boundary lubrication regime. The friction coefficient, lubrication lifetime, and species evolved from the liquid lubricant by tribodegradation can be determined. A complete analysis of the contact stresses and energy dissipation together with experimental evidence supporting the analysis are presented.

14. SUBJECT TERMS

Vacuum tribology; Liquid lubricants; Rolling contacts; Boundary lubrication; Contact mechanics

15. NUMBER OF PAGES

19

16. PRICE CODE

A03

17. SECURITY CLASSIFICATION OF REPORT	18. SECURITY CLASSIFICATION OF THIS PAGE	19. SECURITY CLASSIFICATION OF ABSTRACT	20. LIMITATION OF ABSTRACT
Unclassified	Unclassified	Unclassified	